JOURNAL OF BACTERIOLOGY, Dec. 2003, p. 6773–6779 Vol. 185, No. 23
0021-9193/03/$08.00+0 DOI: 10.1128/JB.185.23.6773–6779.2003

Identification and Characterization of the Nickel Uptake System for Urease Biogenesis in *Streptococcus salivarius* 57.I

Yi-Ywan M. Chen and Robert A. Burne*

Department of Oral Biology, University of Florida, Gainesville, Florida 32610

Received 8 September 2002/Accepted 14 September 2003

Ureases are multisubunit enzymes requiring Ni^{2+} for activity. The low pH-inducible urease gene cluster in *Streptococcus salivarius* 57.I is organized as an operon, beginning with *ureI*, followed by *ureABC* (structural genes), and *ureEFGD* (accessory genes). Urease biogenesis also requires a high-affinity Ni^{2+} uptake system. By searching the partial genome sequence of a closely related organism, *Streptococcus thermophilus* LMG18311, three open reading frame (ORFs) homologous to those encoding proteins involved in cobalamin biosynthesis and cobalt transport (*cbiMQO*) were identified immediately 3′ to the *ure* operon. To determine whether these genes were involved in urease biogenesis by catalyzing Ni^{2+} uptake in *S. salivarius*, regions 3′ to *ureD* were amplified by PCRs from *S. salivarius* by using primers identical to the *S. thermophilus* sequences. Sequence analysis of the products revealed three ORFs. Reverse transcriptase PCR was used to demonstrate that the ORFs are transcribed as part of the *ure* operon. Insertional inactivation of ORF1 with a polar kanamycin marker completely abolished urease activity and the ability to accumulate $^{63}Ni^{2+}$ during growth. Supplementation of the growth medium with $NiCl_2$ at concentrations as low as 2.5 μM partially restored urease activity in the mutant. Both wild-type and mutant strains showed enhanced urease activity when exogenous Ni^{2+} was provided at neutral pH. Enhancement of urease activity by adding nickel was regulated at the posttranslational level. Thus, ORF1, ORF2, and ORF3 are part of the *ure* operon, and these genes, designated *ureM*, *ureQ*, and *ureO*, respectively, likely encode a Ni^{2+}-specific ATP-binding cassette transporter.

Ureases are Ni^{2+}-requiring metallo-enzymes that have been isolated and characterized from a variety of prokaryotes and eukaryotes (21). The production of ammonia and CO_2 from urea hydrolysis by urease has been shown to have a major impact on microbial pathogenesis (4). Genes required for the biogenesis of bacterial ureases are generally arranged as operons, with the structural genes: *ureC*, *ureB*, and *ureA*, encoding the α, β, and γ subunits, respectively, followed by the accessory genes: *ureE*, *ureF*, *ureG*, and *ureD*, encoding proteins essential for the incorporation of Ni^{2+} into the metallocenter. Other genes, such as *ureI*, encoding urea transporters, are found in the urease operons of *Helicobacter pylori* and *Streptococcus salivarius* (9, 29). Although Ni^{2+} is an essential cofactor for the catalytic activity of urease, most known *ure* operons do not contain genes encoding proteins for Ni^{2+} transportation. One possible exception is *ureH* of *Bacillus* sp. strain TB-90 (20), which shares homology with the high-affinity nickel-specific permease encoded by *hoxN* of *Ralstonia eutropha* (12).

Nickel is usually present in trace amounts in the natural environment and is crucial for a number of biological processes, such as hydrolysis of urea, consumption of molecular hydrogen, and methanogenesis. Free nickel is toxic (28); therefore, nickel-specific transporters usually display high affinity but low capacity, presumably to guard against potential toxic effects caused by high levels of intracellular nickel. Thus far, two distinct high-affinity nickel transport systems have been described in prokaryotes: the single-component Ni^{2+} permeases, which belong to the nickel/cobalt transporter (NiCoT) family, and the Nik systems, which belong to the ATP-dependent binding cassette (ABC) transporter family (14). The most studied, single-component Ni^{2+}-specific permease is HoxN from *R. eutropha* (13, 15, 30). Similar systems have been identified in other bacteria, including HupN from *Bradyrhizobium japonicum* (16), NixA from *H. pylori* (17), and possibly UreH from *Bacillus* sp. *strain* TB-90 (20).

The Nik system was originally identified in *Escherichia coli* and is composed of one periplasmic Ni^{2+} binding protein (NikA), two hydrophobic transmembrane proteins, NikB and NikC, which are assumed to form the channel for Ni^{2+} uptake, and two membrane-associated components, NikD and NikE, which contain the conserved signature sequences of ATPases and are believed to be involved in the energy-coupling process for transport (22). The expression of the *E. coli nik* operon is negatively regulated at the transcriptional level by the NikR repressor protein when intracellular nickel levels are high (11). Similar Ni^{2+} uptake systems have been identified in *Brucella suis* (18), *Vibrio parahaemolyticus* (23), *Actinobacillus pleuropneumoniae* (2), and *Yersinia pseudotuberculosis* (25), and in all cases this Ni^{2+}-specific transporter is associated with ureolytic activity of the microorganisms.

S. salivarius is one of the most abundant and highly ureolytic microorganisms in the oral cavity and can use urea as a primary source of nitrogen (5). The expression of urease in *S. salivarius* is subject to environmental signals, with higher levels of expression in cells grown under acidic conditions, and the induction at acidic pH values can be enhanced by growth in excess amounts of carbohydrate (6). It is believed that regulation by low pH and carbohydrate availability allows for maximal production of the enzyme when it is most needed for survival of the organisms against lethal acidification (5). The urease gene

* Corresponding author. Mailing address: Department of Oral Biology, University of Florida, 1600 SW Archer Rd., P.O. Box 100424, Gainesville, FL 32610. Phone: (352) 392-4370. Fax: (352) 392-7357. E-mail: rburne@dental.ufl.edu.

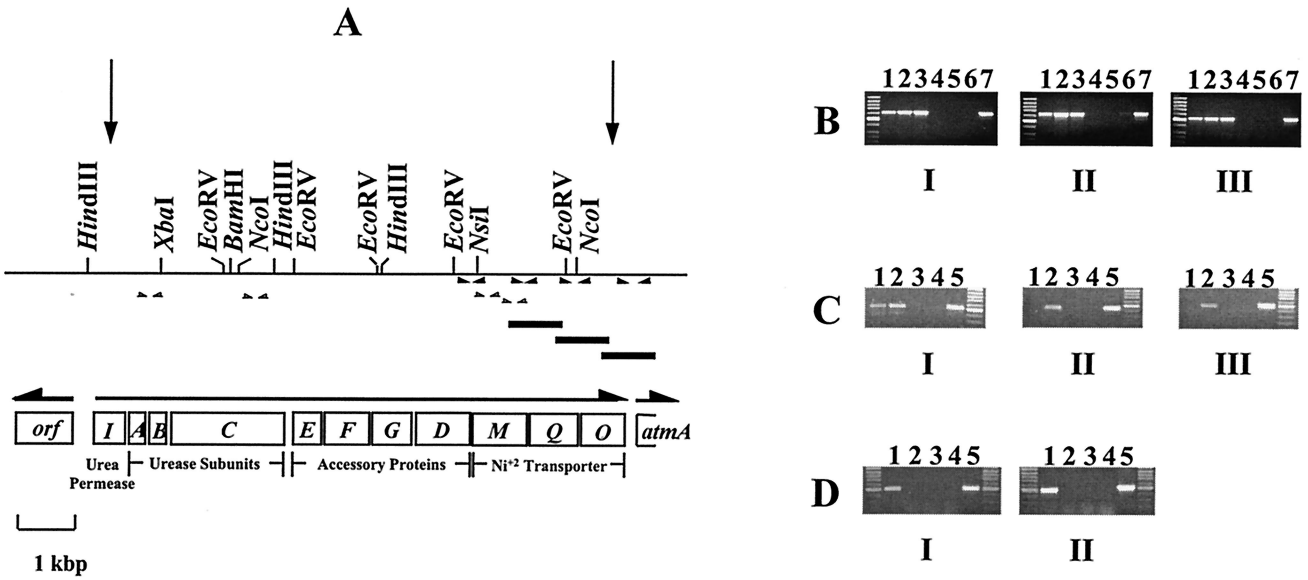

FIG. 1. (A) Schematic diagram of the *ure* operon of *S. salivarius* 57.I. A restriction endonuclease map of the chromosome containing the *ure* cluster is shown on the top line. The relative locations and sizes of each ORF are indicated. The directions of transcription of the *ure* operon and flanking genes are indicated by horizontal arrows. The limits of the partial *ure* cluster in *S. mutans* ACUS6 are indicated by vertical arrows. The locations and orientations of primer pairs used in RT-PCR for detecting contiguous mRNA between *ureM*, *ureQ*, and *ureO*, and for detecting *ureAB*-, *ureC*-, or *ureM*-specific mRNAs are indicated by solid and by open horizontal arrows, respectively, immediately under the restriction map. Below, the locations of the PCR products are shown in solid lines. (B) PCR products generated from RT-PCR. A total of 10% of the total cDNA generated by RT-PCR from each RNA sample was amplified with specific primers (see panel A), and 10% of the total PCR products were run on a 1.2% Tris-acetate-EDTA gel. Subpanels: I, PCR products generated with a primer pair specific for the *ureDM* intergenic region; II, products generated with a primer pair specific for the *ureMQ* intergenic region; III, products generated with a primer pair specific for the *ureQO* intergenic region. In lanes 1, 2, and 3 RT was included in the reactions; lanes 4, 5, and 6 show the results control reactions that were carried out identically to the experimental samples, but without RT. In lane 7, PCR was used to amplify the target region from *S. salivarius* 57.I chromosomal DNA. Lanes 1 and 4, products generated from cells grown in BHI-KPB; lanes 2 and 5, products from cells grown in BHI; lanes 3 and 6, products from cells grown in BHI-HCl. The 100-bp DNA ladder (MBI Fermentas) was used as the molecular weight marker. (C) PCR products generated from RT-PCR. A total of 10% of total cDNA generated by RT-PCR from each RNA sample was amplified with specific primers (see panel A), and 10% of the total PCR products were run on a 0.8% Tris-acetate-EDTA gel. Lanes 1 and 3, products from an *S. salivarius* strain containing a polar insertion mutation in the *ureC* gene (5); lanes 2 and 4, products from wild-type *S. salivarius.* In lanes 1and 2, RT was included in the reactions; in lanes 3 and 4 were control reactions without RT. In lane 5, the PCR product was amplified from *S. salivarius* 57.I chromosomal DNA. Subpanels: I, PCR products generated with a pair primer specific for *ureAB* region; II, products generated with a primer pair specific for the *ureC*; III, products generated with a primer pair specific for the 3′ half of *ureM* (ORF1). Ladder mix DNA ladder (MBI Fermentas) was used as the molecular weight marker. (D) PCR products generated from RT-PCR. A total of 10% of total cDNA generated by RT-PCR from each RNA sample was amplified with specific primers (see panel A), and 20% of the total PCR products were run on a 0.8% Tris-acetate-EDTA gel. Subpanels: I, PCR products were generated with a primer pair located immediately 3 to the Ω*kan* insertion; II, products generated with a primer pair located 500 bp 3′ to the ATG start condon of *ureM.* In lanes 1 and 2, RT was included in the reactions; lanes 3 and 4 were controls without RT. In lane 5, the sample was PCR amplified from *S. salivarius* 57.I chromosomal DNA. The same DNA ladder was used as in panel B.

cluster (*ure*) of *S. salivarius* is arranged as an operon, beginning with *ureI*, followed by *ureABCEFGD* (9). Previous studies indicated that *ureABCEFGD* are required for assembly of a functional urease. However, a recombinant *Streptococcus mutans* strain (ACUS6) harboring only the 3′ portion of *ureI*, starting at the sequence encoding the 65th amino acid of the deduced UreI, and intact *ureABCEFGD* (10) (Fig. 1A) requires supplementation with $NiCl_2$ to produce an active urease enzyme. The purpose of the present study was to identify genes involved in nickel uptake by *S. salivarius.*

MATERIALS AND METHODS

Bacterial strains, growth conditions, and reagents. *S. salivarius* 57.I and its UreMQO-deficient derivative were routinely grown in brain heart infusion (BHI; Difco Laboratories) at 37°C in 5% CO_2 and 95% air. Recombinant *E. coli* strains were routinely maintained in L broth. Kanamycin was included in the growth medium, when indicated, at 750 or 50 μg ml^{-1} for recombinant *S. salivarius* or *E. coli* strains, respectively. All chemical reagents and antibiotics were purchased from Sigma. $^{63}NiCl_2$ (9.87 mCi of Ni mg^{-1}) was purchased from Amersham Biosciences (Piscataway, N.J.). To obtain cultures grown under neutral or acidic conditions, cells were grown in BHI containing 50 mM potassium phosphate buffer (pH 7.4; BHI-KPB), BHI alone, or BHI that had been adjusted to pH 5.8 by the addition of 2 N HCl (BHI-HCl).

Nucleic acid manipulations. Genomic DNA from *S. salivarius* 57.I was isolated as previously described (8). Plasmid DNA from recombinant *E. coli* strains was purified by using the QIAprep spin plasmid kit (Qiagen, Inc.). Cloning, Southern blot analysis, and hybridizations were carried out by using an established protocol (1). Restriction endonucleases, DNA polymerases, and RNA reverse transcriptase (RT) were obtained from Invitrogen or New England Biolabs (NEB). Total cellular RNA from *S. salivarius* strains was isolated as described elsewhere (9). Levels of *ure*-specific mRNA were quantitated by densitometry using slot blot analysis, with hybridization and washes carried out at high stringency (6).

Isolation of *ureM*, *ureQ*, and *ureO*. The region immediately 3′ to the *ure* cluster was amplified from *S. salivarius* 57.I by PCRs with primers derived from the *Streptococcus thermophilus* LMG18311 genome sequences (http://www.biol.ucl.ac.be/gene/genome/). PCRs were initiated with five cycles at a less stringent annealing temperature (50°C), followed by 20 cycles at a more stringent annealing temperature (55°C). All PCR products were cloned onto plasmid pCRII (Invitrogen) and the sequences were determined.

Construction of a UreMQO-deficient *S. salivarius*. A *Hin*dIII-*Nco*I fragment, 2.9 kbp in size, containing the 3′ portion of *ureG*, *ureD* through *ureM*, and the 5′

portion of *ureQ* (Fig. 1A) was initially subcloned from pMC11 (8) into pGEM3Zf(+) to generate plasmid pMC281. A DNA fragment containing a kanamycin resistance marker flanked by transcription/translation terminators (Ω*kan*) (24) was subsequently cloned into the unique *Nsi*I site, located at the beginning of *ureM*, on plasmid pMC281. The resulting chimeric plasmid, pMC282, was transferred into strain 57.I by electroporation (9) to introduce a polar mutation in *ureM* by allelic exchange. The configuration of the double-crossover integration of the kanamycin resistance marker was confirmed by PCR and Southern blot analysis.

Nickel accumulation. A nickel accumulation assay was adopted from Wolfram et al. (30) with minor modifications. Briefly, overnight cultures of *S. salivarius* strains in BHI were diluted 1:50 into fresh BHI-KPB or BHI containing 500 nM $^{63}NiCl_2$. Unlabeled metal chlorides as competitors were added to a final concentration of 5 μM. All cultures were grown at 37°C for 5 h at which point the optical density at 600 nm (OD_{600}) of the cultures was ca. 0.9. Cells were harvested, washed twice with an equal volume of ice-cold buffer A (50 mM Tris-HCl, 10 mM $MgCl_2$ [pH 7.5]), and then concentrated 10-fold in the same buffer. The radioactivity of an aliquot of the cell suspension (100 μl) was determined by liquid scintillation counting. To monitor the amount of $^{63}Ni^{2+}$ accumulated intracellularly over time, cells were grown in BHI at 37°C for 3 h and 45 min prior to addition of $^{63}NiCl_2$. A 1-ml aliquot of the cell suspension was harvested every 15 min after addition and processed as described above. The CFU count in the same amount of cell suspension was determined by serial dilution and plating on BHI agar plates. Alternatively, the same amount of cell suspension was subjected to mechanical disruption in the presence of glass beads (0.1 mm in diameter) by homogenization in a Bead Beater (Biospec Products) for a total of 40 s at 4°C. The concentration of each cell lysate was determined by using the Bio-Rad protein assay based on the method of Bradford (3). The cellular content of $^{63}NiCl_2$ was expressed in picomoles per 10^9 CFU or picomoles per milligram of protein.

Urease assays. Overnight cultures of the wild-type *S. salivarius* 57.I and its UreMQO-deficient derivative were diluted 1:20 into fresh BHI-KPB, BHI, or BHI-HCl containing 0, 2.5, 5, 10, 25, 50, 75, or 100 μM $NiCl_2$ and grown to an OD_{600} of ~0.65. Cultures were harvested by centrifugation, washed once with an equal volume of 10 mM KPB (pH 7.0), and then concentrated 40-fold in the same buffer. Concentrated cell suspensions were subjected to mechanical disruption as described above. Urease activity was measured as described previously (6) and normalized to the protein concentration.

RESULTS AND DISCUSSION

Isolation and sequence analysis of *ureM*, *ureQ*, and *ureO*. Urease biogenesis by bacteria requires a high-affinity Ni^{2+} uptake system. By searching the partial genome sequence of a closely related, ureolytic organism, *S. thermophilus* LMG18311, three open reading frames (ORFs) related to those encoding proteins similar to the ABC-type cobalt transport system found in cobalamin biosynthesis operons (*cbiMQO*) were identified immediately 3′ to the *ure* operon. To determine whether these genes were present in *S. salivarius*, a chromosome walking approach was used to obtain sequences 3′ to *ureD* by PCRs from *S. salivarius* with primers identical to the *cbiM*, *cbiQ*, and *cbiO* genes of *S. thermophilus*. Approximately 3 kbp of sequence immediately 3′ to *ureD* was obtained from the three overlapping PCR products (Fig. 1A). Three complete ORFs and an additional partial ORF, all in the same orientation as the *ure* operon, could be identified within this 3-kbp region. ORF1, with its ribosome binding site embedded in *ureD*, is located three bases 3′ to the stop codon of *ureD*. ORF2 overlaps with ORF1 by two bases, and ORF3 is located one base 3′ to ORF2. The partial ORF is located 165 bp 3′ to ORF3. To determine whether these ORFs were cotranscribed with the *ure* operon, RT-PCR was used to detect the existence of contiguous transcripts between *ureD*, ORF1, ORF2, and ORF3. The results indicated the presence of contiguous transcript(s) between *ureD*, ORF1, ORF2, and ORF3, suggesting that all three ORFs could be cotranscribed with the urease genes and were part of the *ure* operon (Fig. 1B). To determine whether ORF1, ORF2, and ORF3 could be transcribed independently, presumably via a promoter embedded somewhere within the *ureI-D* genes, total cellular RNA was isolated from a recombinant *S. salivarius* strain in which *ureC* had been insertionally inactivated by allelic exchange (5), and the presence of ORF1-specific mRNA was determined by RT-PCR (Fig. 1C). When a polar mutation was introduced into *ureC*, no detectable ORF1-specific transcript was observed by RT-PCR, indicating ORF1, ORF2, and ORF3 were transcribed exclusively from the promoter 5′ to *ureC*. A polar insertion in *ureI* also resulted in no detectable ORF1 transcript by RT-PCR (data not shown). A stable stem-loop structure, with $\Delta G^\circ = -10.3$ kcal, followed by a stretch of six T residues, which could potentially function as a rho-independent terminator, was identified seven bases 3′ to the stop codon of ORF3, and no transcript could be detected by RT-PCR between ORF3 and the partial downstream ORF (data not shown), a finding indicating that this partial ORF is not part of the *ure* operon. The sequence of this partial ORF encoded a truncated peptide that shared significant homology (60 to 70% identity) with the N terminus of the substrate-binding proteins of amino acid ABC-type transporters (AtmA) from other streptococcal species. The lack of involvement of this ORF in urea metabolism was further confirmed by demonstrating that there was no change in urease activity in a recombinant strain in which this ORF was insertionally inactivated (data not shown). ORF1, ORF2, and ORF3 were designated *ureM*, *ureQ*, and *ureO*, respectively, and it was concluded that the *ure* operon of *S. salivarius* 57.I consists of 11 genes (*ureIABCEFGDMQO*). The complete sequence of the *ure* operon has been deposited with GenBank under accession number U35248.

Even though utilizing an ABC-type Ni uptake system for urease biogenesis is not unique to *S. salivarius*, the organization of the *ure* operon of this organism is different from that of other urease-producing bacteria. Specifically, all other known bacterial ABC-type nickel uptake systems that are associated with urease biogenesis are encoded by separate operons, e.g., the *nik* or *cbi* operons, and the expression of these operons is generally regulated independently from *ure* operons (2, 18).

Translation of *S. salivarius ureM* predicted a protein of 325 amino acids with a pI of 8.99 and a calculated mass of 35.2 kDa. UreM shared significant degrees of similarity with CbiM, which has been suggested to encode an integral membrane protein involved in cobalt transport for cobalamin biosynthesis, from *Thermoanaerobacter tengcongensis* (47% identity and 64% similarity) and *Clostridium acetobutylicum* (39% identity and 58% similarity). The conserved domain of the permease component of ABC-type Co^{2+} transport systems could also be identified within UreM, and three transmembrane helices were predicted by using CBS prediction services (Center for Biological Sequence Analysis, Technical University of Denmark, Lyngby, Denmark [http://www.cbs.dtu.dk/services/]). *S. salivarius ureQ* (777 nucleotides) encoded a 29.1-kDa protein with a pI of 9.63. The highest degree of similarity was observed between *ureQ* and genes predicted to encode cobalt permeases from *Lactobacillus plantarum* (28% identity and 43% similarity) and from *C. acetobutylicum* (24% identity and 46% similarity). Eight transmembrane helices were predicted in deduced UreQ sequence by using CBS prediction services. *S. salivarius ureO*

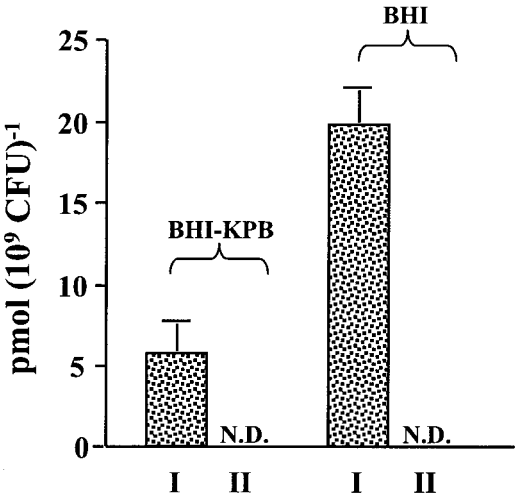

FIG. 2. $^{63}Ni^{2+}$ accumulation in *S. salivarius* 57.I and UreMQO-deficient strains. Columns: I, wild-type *S. salivarius*; II, UreMQO-deficient strain. Values are the means and standard deviations of four independent samples. N.D., not detectable.

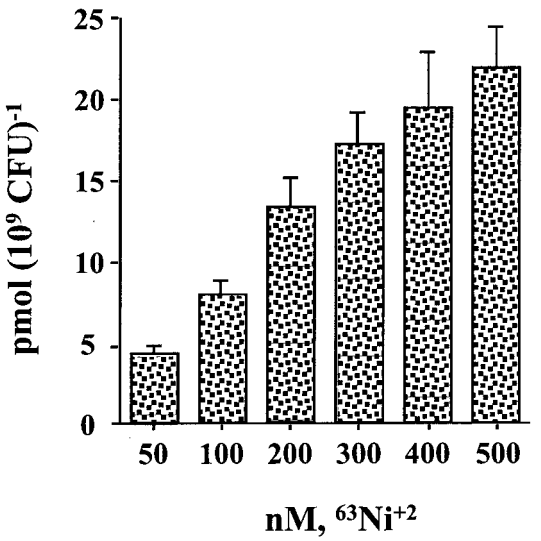

FIG. 3. Concentration-dependent nickel accumulation in *S. salivarius.* Values are the means and standard deviations of four independent samples.

(714 nucleotides) encoded a 27.6-kDa protein with a pI of 5.44. UreO shared 44, 40, and 37% identity to the ATPase components of ABC-type cobalt transport systems (CbiO) of *L. plantarum*, *C. acetobutylicum*, and *T. tengcongensis*, respectively. Significant levels of similarity to the ATP-binding proteins of cobalt ABC transporters from *Methanosarcina* species were also observed (35% identity). The linker peptide (LSGGEKKK), and the Walker A (GENGTGKS) and Walker B (VYILD) motifs commonly found in many ATP- and GTP-binding and hydrolyzing proteins were also observed in the correct respective positions in the protein.

Functional analysis of UreMQO in Ni^{2+} accumulation. To examine the impact of UreMQO in urease biosynthesis, a polar mutation (Ω*kan*) was introduced into *ureM*, four bases 3′ to the ATG start codon. To ensure that the transcription of the urease operon terminated at the position of Ω*kan*, total RNA was isolated from *S. salivarius* wild-type and UreMQO-deficient strains, and RT-PCR was used to detect *ureM*-specific mRNA (Fig. 1D). No RT-PCR product could be detected 3′ to Ω*kan*.

Earlier studies demonstrated that urease expression in *S. salivarius* is predominantly regulated by growth pH (6, 9). At neutral pH, expression is almost completely repressed. Induction occurs and increases as the growth pH becomes more acidic. To determine whether the capacity to accumulate Ni^{2+} in both wild-type and UreMQO-deficient strains was also regulated by pH, cells were cultured in BHI-KPB or in BHI as described in Materials and Methods to late-exponential phase, at which point the cultures were at approximately pH 7.0 and 5.5, respectively. When cells were incubated with 500 nM $^{63}NiCl_2$, it was found that $^{63}Ni^{2+}$ accumulation was ca. 3.5-fold higher in the wild-type organisms that were cultured in acidic medium compared to those grown in neutral medium (Fig. 2). In contrast, $^{63}Ni^{2+}$ accumulation in the UreMQO-deficient strain was abolished, indicating that UreMQO are essential for the uptake of $^{63}Ni^{2+}$ from the environment. The accumulation of $^{63}Ni^{2+}$ in wild-type *S. salivarius* during growth was further confirmed by incubating the cells with different amounts of $^{63}Ni^{2+}$, and it was found that the amount of intracellular $^{63}Ni^{2+}$ was a direct result of the concentrations of exogenous of $^{63}Ni^{2+}$ (Fig. 3).

The substrate specificity of UreMQO in wild-type *S. salivarius* was examined by the addition of unlabeled Co^{2+}, Zn^{2+}, Mn^{2+}, Mg^{2+}, and Ni^{2+} at a 10-fold excess (5 μM) in growth medium containing 500 nM $^{63}Ni^{2+}$. It was found that excess amounts of unlabeled Co^{2+}, Zn^{2+}, Mn^{2+}, or Mg^{2+} chloride did not result in a significant decrease in the amount of $^{63}Ni^{2+}$ accumulated (Fig. 4). However, the inclusion of 5 μM unlabeled $NiCl_2$ in the growth medium inhibited the accumulation

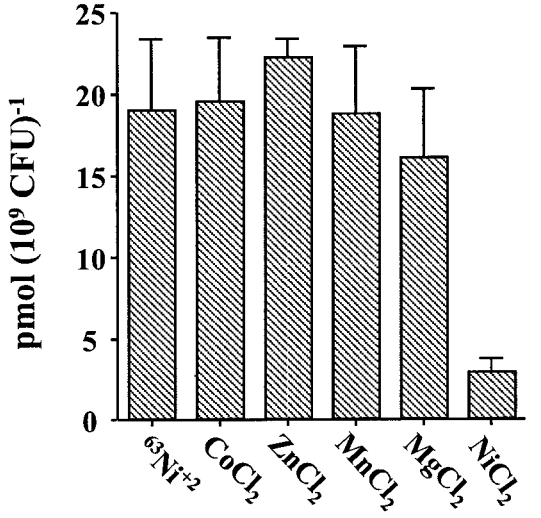

FIG. 4. UreMQO is specific for nickel uptake. Wild-type *S. salivarius* was grown in BHI containing 500 nM $^{63}Ni^{2+}$ alone or with 5 μM unlabeled metal chloride. Values are the means and standard deviations of four independent samples.

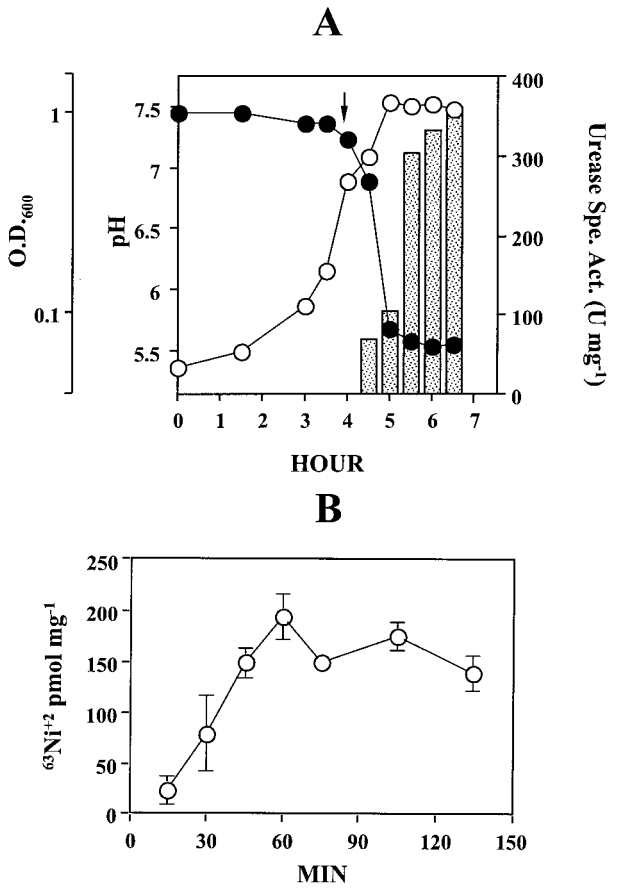

FIG. 5. (A) Growth, urease expression, and culture pH versus time. The pH values (●) and the OD_{600} (○) of batch cultures of wild-type *S. salivarius* in BHI are shown. The urease specific activities of cultures were determined every 30 min beginning at 4 h and 30 min postinoculation. The specific activities are expressed as nanomoles of urea hydrolyzed per minute per milligram of protein. The time at which $^{63}Ni^{2+}$ was added to the cultures in the nickel accumulation time course study is indicated by a vertical arrow. (B) Nickel accumulation in late-exponential phase *S. salivarius.* Values are the means and standard deviations of four independent samples.

of $^{63}Ni^{2+}$ by 85%, indicating that UreMQO have specificity for Ni^{2+} ion.

Initial attempts to determine the kinetic parameter of UreMQO in nickel transport by using standard transport assays were unsuccessful, presumably due to the low transport capacity of the system and a high level of nonspecific binding of the Ni^{2+} to the cell surface. To circumvent this limitation, we used a modified accumulation assay in a time course study, in which a larger size of cell suspension was collected by centrifugation at each time point, followed by two washes with buffer containing 10 mM Mg^{2+} to remove nonspecifically bound $^{63}Ni^{2+}$. It was found that the expression of the *S. salivarius* urease operon, which is tightly regulated by growth pH (7), was repressed until the pH of the culture reached ~6.5, at which time the urease specific activity increased linearly and peaked during the late exponential phase of growth (Fig. 5A). To ensure that nickel accumulation was monitored during biogenesis of an active urease, $^{63}Ni^{2+}$ was added to the cultures at 3 h and 45 min postinoculation, and the amount of $^{63}Ni^{2+}$ was monitored every 15 min afterward. A time-dependent accumulation was observed, and the accumulation reached maximal levels 60 min after the addition of $^{63}Ni^{2+}$ (Fig. 5B). No significant uptake of nickel occurred prior to the induction of the urease operon (data not shown).

Urease activity was enhanced by exogenous $NiCl_2$. It is known that the average concentration of nickel in the natural environment is in the nanomolar range and that the most commonly occurring oxidation state of nickel is Ni(II). When Ni^{2+} is present at higher concentrations, it can be transported by Mg^{2+} transport systems (19, 26). To determine the influence of UreMQO in overall urease biosynthesis and whether high concentrations of exogenous Ni^{2+} could compensate for the deficiency of the Ni^{2+}-specific uptake system, possibly through a Mg^{2+} uptake system, urease activities were examined in wild-type and UreMQO-deficient strains at different growth pH values, with or without additional $NiCl_2$ (Fig. 6). No detectable urease activity was observed in the UreMQO-deficient strain in the absence of supplemented $NiCl_2$, regardless of the growth pH. When cells were grown at neutral pH, supplementation with as little as 2.5 μM $NiCl_2$ was able to partially restore the ureolytic phenotype in the UreMQO-deficient strain, and the levels of urease activity increased in a $NiCl_2$ concentration-dependent manner. $NiCl_2$-dependent increases in urease activity were also observed in cells grown in BHI and BHI-HCl, and the highest levels of urease activity at each $NiCl_2$ concentration supplied to the system were consistently observed in cells grown in BHI-HCl. In the absence of exogenous $NiCl_2$, urease activity in the wild-type strain was solely regulated by growth pH, with the highest urease activity observed in cells grown in BHI-HCl.

Interestingly, when cells were grown at neutral pH (BHI-KPB), urease activity in the wild-type cells increased in response to increasing concentrations of $NiCl_2$, and the enhancement by $NiCl_2$ reached saturation at 25 μM. The enhancement of urease activity by $NiCl_2$ was less prominent when cells were grown at acidic pH. When cells were grown in BHI without any buffer, the highest level of activation by $NiCl_2$ occurred at 2.5 μM, but there was no significant increase in urease activity with higher concentrations of $NiCl_2$ when cells were grown in BHI-HCl. Therefore, under conditions in which the *ureMQO* may not be fully induced, the addition of nickel can increase the amount of activated urease, suggesting that nickel uptake is a limiting factor in urease biogenesis at a neutral pH. Under acidic conditions, when expression of the operon is optimal, the accumulation of intracellular Ni^{2+} via the activity of UreMQO appears to be sufficient for the activation of all translated urease subunits, and additional nickel had no impact on the levels of urease activity. Utilizing the capacity of nickel accumulation as a limiting factor for total urease activity at neutral pH provides an additional level of control for urease expression in *S. salivarius*.

Upregulation of urease activity by $NiCl_2$ was regulated at the level of enzyme activation. The expression of urease genes and urease activity in *H. pylori* is regulated by the availability of nickel (27) and supplementation the growth medium with micromolar levels of $NiCl_2$ leads to higher levels of transcription of the operon. To investigate whether the upregulation of urease activity by $NiCl_2$ in *S. salivarius* could be mediated at the level of urease gene transcription from p_{ureI}, the level of ex-

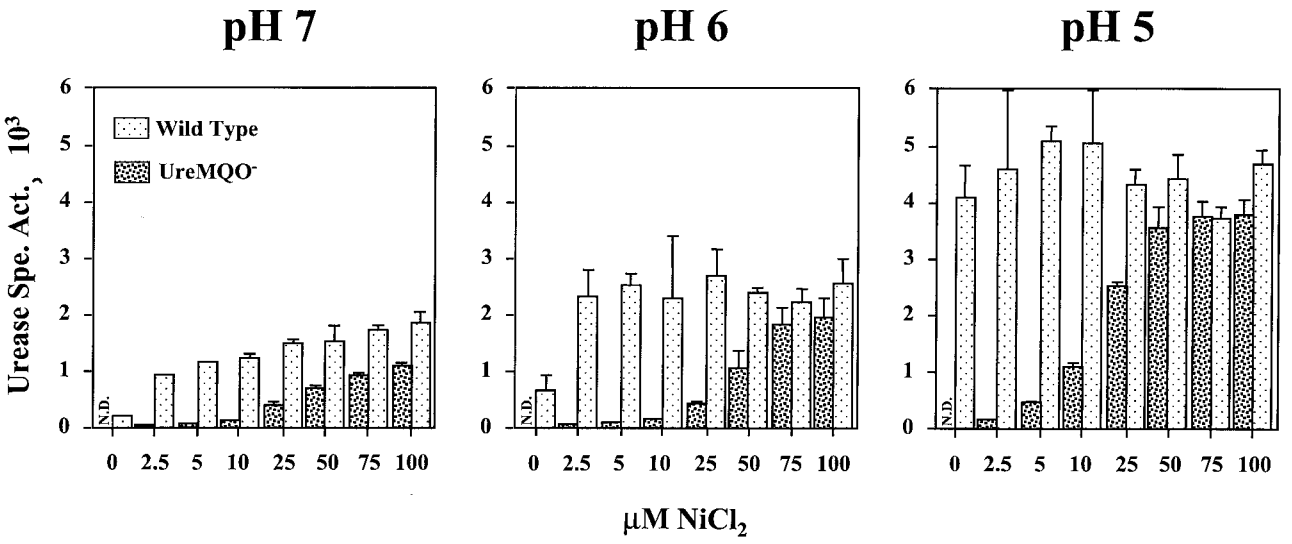

FIG. 6. Urease specific activities in *S. salivarius* 57.I and the UreMQO-deficient strain growing in BHI-KPB, BHI, and BHI-HCl containing 0 to 100 μM $NiCl_2$. The specific activities are expressed as nanomoles of urea hydrolyzed per minute per milligram of protein. The values shown are averages from multiple reaction sets from three independent samples. For each value reported, separate reaction sets with various times and cell quantities, which fell within the linear ranges of the standard curve, were used. All reactions were performed in triplicate. N.D., not detectable.

pression was monitored in the recombinant *S. salivarius* strain *PureIcat*, which carries a single copy of the p_{ureI}-*cat* fusion at the *lacZ* locus (7), by measuring chloramphenicol acetyltransferase (CAT) specific activity. No significant differences in CAT activity were observed in cells grown in different concentrations of $NiCl_2$, regardless of the growth pH (data not shown), confirming that higher levels of urease activity in the presence of $NiCl_2$ did not result from elevated levels of *ure* transcription.

To further confirm that urease gene transcription was not regulated by $NiCl_2$ in *S. salivarius*, total cellular RNA was isolated from wild-type cells and the UreMQO-deficient strain grown in BHI-KPO_4 that was supplemented with 0 to 100 μM $NiCl_2$ and the amounts of *ureC*- and *ureM*-specific mRNA were quantitated by slot blot analysis. No significant difference in the levels of *ureC*-specific mRNA could be detected in the wild-type strain under all concentrations of $NiCl_2$ tested (Fig. 7). Likewise, no differences in *ureC*-specific mRNA were detected between the wild-type and UreMQO-deficient strains in response to nickel concentrations, indicating that the nickel-responsive activation of urease activity is not mediated at the transcriptional level. As expected, the levels of *ureM*-specific message in the wild-type strain were not influenced by the amount of $NiCl_2$ in the growth medium (Fig. 7), and there was no detectable *ureM* signal in the UreMQO-deficient strain (data not shown).

To determine whether posttranscriptional regulation is a factor in the enhancement of urease activity by exogenous $NiCl_2$, we also examined the levels of UreC protein, the α subunit of the urease enzyme, by Western blot analysis with an anti-UreC polyclonal antibody in strains grown in different concentrations of $NiCl_2$. No significant differences in the levels of UreC were noted in the wild-type or UreMQO-deficient strains in response to the amount of $NiCl_2$ added to the medium (data not shown). These results indicate that the absence

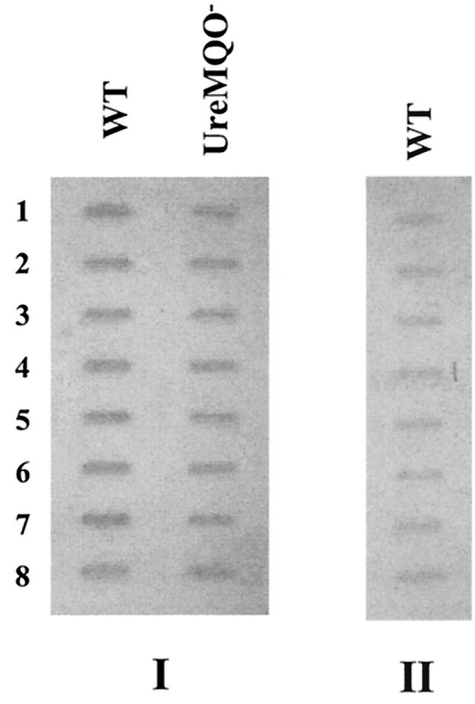

FIG. 7. Slot blot analysis of *ureC*- and *ureM*-specific mRNA. Total cellular RNA of wild-type 57.I and UreMQO-deficient strains was isolated as described previously (9) and further purified by using the RNeasy total RNA kit (Qiagen). Panels: I, 10 μg of total RNA probed with a *ureC*-specific probe; II, 20 μg of total RNA probed with a *ureM*-specific probe. Columns 1 to 8 represent RNA isolated from cells grown in BHI-KBP supplemented with 0, 2.5, 5, 10, 25, 50, 75, and 100 μM $NiCl_2$, respectively. Negative controls are 10 μg of total cellular RNA treated with RNase A prior to loading.

of detectable urease activity in the UreMQO-deficient strains in the absence of exogenous $NiCl_2$ was due to the inability to transport $NiCl_2$ in the mutant rather than the lack of production of urease subunits and, again, that $NiCl_2$ does not regulate urease expression at the level of transcription or translation.

Summary. In conclusion, *S. salivarius* possess a multicomponent nickel transporter belonging to the ABC transporter superfamily. In contrast to most pathogenic microorganisms, which generally possess more than one nickel uptake systems for all nickel-requiring enzymes, UreMQO is likely to be the only nickel-specific uptake system in *S. salivarius*. Nevertheless, other metal transport systems, presumably magnesium transporters, could also transport nickel when this metal was supplied in excess.

ACKNOWLEDGMENT

This work was supported by Public Health Service grant DE10362 from the NIDCR to R.A.B.

REFERENCES

1. **Ausubel, F. M., R. Brent, R. E. Kingston, D. D. Moore, J. G. Seidman, J. A. Smith, and K. Struhl.** 1989. Current protocols in molecular biology. John Wiley & Sons, Inc., New York, N.Y.
2. **Bosse, J. T., H. D. Gilmour, and J. I. MacInnes.** 2001. Novel genes affecting urease activity in *Actinobacillus pleuropneumoniae.* J. Bacteriol. **183:**1242–1247.
3. **Bradford, M. M.** 1976. A rapid and sensitive method for the quantitation of microgram quantities of protein utilizing the principle of protein-dye binding. Anal. Biochem. **72:**248–254.
4. **Burne, R. A., and Y. M. Chen.** 2000. Bacterial ureases in infectious diseases. Microbes Infect. **2:**533–542.
5. **Chen, Y. M., C. A. Weaver, and R. A. Burne.** 2000. Dual functions of *Streptococcus salivarius* urease. J. Bacteriol. **182:**4667–4669.
6. **Chen, Y. M., and R. A. Burne.** 1996. Analysis of *Streptococcus salivarius* urease expression using continuous chemostat culture. FEMS Microbiol. Lett. **135:**223–229.
7. **Chen, Y. M., M. J. Betzenhauser, and R. A. Burne.** 2002. *cis*-Acting elements that regulate the low-pH-inducible urease operon of *Streptococcus salivarius.* Microbiol. **148:**3599–3608.
8. **Chen, Y. M., K. A. Clancy, and R. A. Burne.** 1996. *Streptococcus salivarius* urease: genetic and biochemical characterization and expression in a dental plaque streptococcus. Infect. Immun. **64:**585–592.
9. **Chen, Y. M., C. A. Weaver, D. R. Mendelsohn, and R. A. Burne.** 1998. Transcriptional regulation of the *Streptococcus salivarius* 57.I urease operon. J. Bacteriol. **180:**5769–5775.
10. **Clancy, K. A., S. Pearson, W. H. Bowen, and R. A. Burne.** 2000. Characterization of recombinant, ureolytic *Streptococcus mutans* demonstrates an inverse relationship between dental plaque ureolytic capacity and cariogenicity. Infect. Immun. **68:**2621–2629.
11. **De Pina, K., V. Desjardin, M. A. Mandrand-Berthelot, G. Giordano, and L. F. Wu.** 1999. Isolation and characterization of the *nikR* gene encoding a nickel-responsive regulator in *Escherichia coli.* J. Bacteriol. **181:**670–674.
12. **Eitinger, T., and B. Friedrich.** 1991. Cloning, nucleotide sequence, and heterologous expression of a high-affinity nickel transport gene from *Alcaligenes eutrophus.* J. Biol. Chem. **266:**3222–3227.
13. **Eitinger, T., and B. Friedrich.** 1994. A topological model for the high-affinity nickel transporter of *Alcaligenes eutrophus.* Mol. Microbiol. **12:**1025–1032.
14. **Eitinger, T., and M. A. Mandrand-Berthelot.** 2000. Nickel transport systems in microorganisms. Arch. Microbiol. **173:**1–9.
15. **Eitinger, T., L. Wolfram, O. Degen, and C. Anthon.** 1997. A Ni^{2+} binding motif is the basis of high affinity transport of the *Alcaligenes eutrophus* nickel permease. J. Biol. Chem. **272:**17139–17144.
16. **Fu, C., S. Javedan, F. Moshiri, and R. J. Maier.** 1994. Bacterial genes involved in incorporation of nickel into a hydrogenase enzyme. Proc. Natl. Acad. Sci. USA **91:**5099–5103.
17. **Fulkerson, J. F., Jr., and H. L. Mobley.** 2000. Membrane topology of the NixA nickel transporter of *Helicobacter pylori*: two nickel transport-specific motifs within transmembrane helices II and III. J. Bacteriol. **182:**1722–1730.
18. **Jubier-Maurin, V., A. Rodrigue, S. Ouahrani-Bettache, M. Layssac, M. A. Mandrand-Berthelot, S. Kohler, and J. P. Liautard.** 2001. Identification of the *nik* gene cluster of *Brucella suis*: regulation and contribution to urease activity. J. Bacteriol. **183:**426–434.
19. **Kehres, D. G., C. H. Lawyer, and M. E. Maguire.** 1998. The CorA magnesium transporter gene family. Microb. Comp. Genomics **3:**151–169.
20. **Maeda, M., M. Hidaka, A. Nakamura, H. Masaki, and T. Uozumi.** 1994. Cloning, sequencing, and expression of thermophilic *Bacillus* sp. strain TB-90 urease gene complex in *Escherichia coli.* J. Bacteriol. **176:**432–442.
21. **Mobley, H. L. T., M. D. Island, and R. P. Hausinger.** 1995. Molecular biology of ureases. Microbiol. Rev. **59:**451–480.
22. **Navarro, C., L. F. Wu, and M. A. Mandrand-Berthelot.** 1993. The *nik* operon of *Escherichia coli* encodes a periplasmic binding-protein-dependent transport system for nickel. Mol. Microbiol. **9:**1181–1191.
23. **Park, K. S., T. Iida, Y. Yamaichi, T. Oyagi, K. Yamamoto, and T. Honda.** 2000. Genetic characterization of DNA region containing the *trh* and *ure* genes of *Vibrio parahaemolyticus.* Infect. Immun. **68:**5742–5748.
24. **Perez-Casal, J., M. G. Caparon, and J. R. Scott.** 1991. Mry, a *trans*-acting positive regulator of the M protein gene of *Streptococcus pyogenes* with similarity to the receptor proteins of two-component regulatory systems. J. Bacteriol. **173:**2617–2624.
25. **Sebbane, F., M. A. Mandrand-Berthelot, and M. Simonet.** 2002. Genes encoding specific nickel transport systems flank the chromosomal urease locus of pathogenic yersiniae. J. Bacteriol. **184:**5706–5713.
26. **Smith, R. L., and M. E. Maguire.** 1998. Microbial magnesium transport: unusual transporters searching for identity. Mol. Microbiol. **28:**217–226.
27. **van Vliet, A. H., E. J. Kuipers, B. Waidner, B. J. Davies, N. de Vries, C. W. Penn, C. M. Vandenbroucke-Grauls, M. Kist, S. Bereswill, and J. G. Kusters.** 2001. Nickel-responsive induction of urease expression in *Helicobacter pylori* is mediated at the transcriptional level. Infect. Immun. **69:**4891–4897.
28. **Von Burg, R.** 1997. Nickel and some nickel compounds. J. Appl. Toxicol. **17:**425–431.
29. **Weeks, D. L., S. Eskandari, D. R. Scott, and G. Sachs.** 2000. A H^+-gated urea channel: the link between *Helicobacter pylori* urease and gastric colonization. Science **287:**482–485.
30. **Wolfram, L., B. Friedrich, and T. Eitinger.** 1995. The *Alcaligenes eutrophus* protein HoxN mediates nickel transport in *Escherichia coli.* J. Bacteriol. **177:**1840–1843.